International Journal of Chemical and Biochemical Sciences
(ISSN 2226-9614)

Journal Home page: www.iscientific.org/Journal.html

The Characteristics of Magnesium Oxide Doped with Silicon Oxide Extracted from Natural Clay as Thermoluminescent Dosimeter

Howa. A. Howash[1], Youssef A. Abdulla*[, 1], Fawzeia Khamis[2], Abdullah Mohd Noh[3]

[1] Faculty of Science, Sebha University, Sebha, Libya, [2] Faculty of Science, Tripoli University, Tripoli, Libya,

[3] Faculty of Health Sciences, Universiti Selangor, Seksyen 7, 40000 Shah Alam, Selangor, Malaysia

Abstract

The SiO_2 nanoparticles have been extracted from clay by the sol-gel method and mixed with magnesium oxide. The $MgOSiO_2$ was characterized by structural characterization using XRD, IR, and XRF. The thermoluminescence properties of the prepared sample were examined using an ultraviolet (UV) source of 254nm. The samples display two peaks at 203°C and 307°C for 0.1% SiO_2 whereas for 0.7% SiO_2, the two peaks appear at 236 °C and 357 °C. The general thermos-luminescent dosimetric characteristics of samples, such as the dose-response, signal fading as a function of storage time, and reproducibility, were also tested using the annealing condition at 400°C for 2 h. The dose-response was linear with UV energy in the range from 100 μJ/cm^2 up to 7700μJ/cm^2 for both concentrations. The coefficient of variation (CV) was found to be 2.3% for 0.1% and about 3.6% for 0.7%. The fading is about 66% in a period of up to 25 days for the 0.1% sample, and for 0.7%, the fading was approximately reduced to 57% of its original value in the same period of 25 days.

Keywords: Thermoluminescence, Clay, MgO, Dosimetry, TL Linearity, Fading

Full length article **Corresponding Author*, e-mail: you.omer@sebhau.edu.ly

1. Introduction

Thermoluminescence has many different meanings over the years, but in the simplest and most modern way, thermoluminescence can be defined as the emission of light from a semiconductor or insulator when it is heated, due to irradiation energy being absorbed and stored [1-2]. Minerals are becoming increasingly important in many industrial areas, including radiation dosimetry, in which thermoluminescence is the most common and most important application. Minerals are usually formed by inorganic processes. The term "clay" refers to a naturally occurring material composed primarily of fine-grained minerals, which is generally plastic at appropriate water content and will harden when dried or fired [3]. With the help of X-ray diffraction, the crystal structures, chemical compositions, particle surface properties, and size distributions of most clay minerals have been considerably revealed. Clay minerals are mostly composed of oxygen, silicon, hydrogen, and aluminum, as well as calcium, sodium, potassium, magnesium, and iron [4]. Recently, studies have been carried out to identify and characterize adequate radiation-sensitive materials that can be used as emergency dosimeters [5]. Egbe et al. study the basic thermoluminescence properties of clay after being subjected to x-rays in the diagnostic energy range.

The results showed very low TL output, but demonstrated enhanced performance with the addition of common salt (NaCl) [6]. These materials are close to the human body composition and are naturally available. Many researchers have been working to separate and employ naturally occurring local materials for the development of thermoluminescence dosimeters (TLD) and other applications. In this regard, many minerals such as feldspar, fluorspar, and quartz have been extensively studied to determine their suitability for such applications [6–10].This study aimed to investigate the structure and thermoluminescence properties of Magnesium Oxide doped with Silicon Oxide after it's subjected to UV energies.

2. Materials and methods

2.1. Sample preparation

2.1.1. Extraction of silica from kaolin clay

Kaolin clay mainly consists of the mineral kaolin, which is a white mineral that represents aluminum silicate. A group of clay samples found in many places in southern Libya that include Sabha, Al-Bawanis, Ubari, and Temsan were collected.

In this study, the clay samples were heated at 680 °C for an hour inside the oven, after grinding the clay and sifting it with a sieve of 0.052 mm in diameter for the purpose of activating silica content in clay. The calcination temperature ranges from 500ºC to 900ºC. Then the samples were weighed and placed in 1000 ml beakers, hydrochloric acid was added at a concentration of 2.5 molarity (10g/100 ml), and the samples were placed on the heater at 90 °C for two hours. The samples were filtered using filter paper and then washed well with distilled water to adjust the pH to 7. NaOH was added at a concentration of 2 M to the samples and placed on the heater for two hours at 90ºC. The samples were filtered and the residues were separated from the filter. The filter, which is sodium silicate, was taken and 10 ml of ethanol was added as a solvent. Then 5 M of nitric acid was added to the samples to get a gel. A centrifuge was used to separate and dispose of the sodium nitrate from the samples at the maximum capacity for 15 minutes. The samples were filtered, washed thoroughly several times with distilled water to get rid of sodium, and dried at 110 °C. Then the samples are heated at 600 °C for 2 hours to obtain nanoparticles of silicon oxide.

2.1.2. Magnesium oxide

Nano-magnesium oxide was prepared by the sol-gel method from magnesium nitrate, EDTA, and citric acid, where each component was mixed separately with distilled water and then they were mixed together in a 1000 ml beaker, the pH of which was adjusted to 7 by ammonia. The sample was placed on the heater until it formed a gel and the burning continued until it changed to black ash. The ash was then placed inside the crucibles for burning in an oven at 600 °C for three hours to get the white powder.

2.1.3. $MgOSiO_2$

A gram of magnesium oxide was added to the silicon oxide sample with two weight concentrations of wt% (0.1, 0.7), mixing each sample with 100 ml of distilled water, placing the samples on the heater at 110^0C until the water evaporates completely (direct burning), then drying at 100^0C for one day. 0.1g of the prepared powder was placed in a cylindrical mold with a diameter of 0.85cm to press about 1.5 tons using a hydraulic press to make a pellet-shaped sample.

2.2. Instrumentation

XRF, XRD, and IR were used to characterize the $MgOSiO_2$ samples. Harshaw Model 3500 TLD Reader was used to test the samples. The glow curves of the samples were estimated from 50ºC to 400ºC at a linear heating rate of 25ºC/sec, the background was subtracted from all results by taking the reading from each sample before irradiation, then subtracts from the reading after irradiation. The samples of 0.1% and 0.7% were irradiated to different UV energies ranging from 100µJ/cm^2 to 7700µJ/cm^2.

3. Results and Discussions

3.1. Material characterization

3.1.1. XRF

The chemical composition analysis using the XRF method revealed the presence of the following elements as oxides (natural clay) which include SiO_2, Al_2O_3, Fe_2O_3, TIO_2, K_2O, CaO, SO_3, and other elements in small amounts. These elements are ordered according to the concentration as shown in **Table 1** for local natural clay, while after the synthesis the amount of SiO_2 reaches 94.1 %. ***3.1.2. FTIR***

The IR spectra of the $MgOSiO_2$ powders produced is presented in **Fig. 1**. The IR band at 3406.47 cm $^{-1}$ are due to the expandable vibration of H_2O molecules. Consistently, an IR band at 1637.27 cm^{-1} was assigned-OH to bend the vibration of H_2O molecules. The shoulder length of 3691.74 cm^{-1} is assigned to the expandable vibration of Si-OH groups in the amorphous structure of SiO_2 [11]. The presence of the Si-OH group is evidence of the formation of integrated water. The strongest and most effective suction peaks in 1061.8 to 1099.1 cm $^{-1}$ of Si-O-Si asymmetric stretching vibrations. The IR band at 956 cm $^{-1}$ can be supplied with silanol groups. The IR band at 800 cm $^{-1}$ can be assigned to the expandable Si-O–Si vibration, while the IR band at 474 cm $^{-1}$ is due to the curved O-Si–O vibration. Previous research revealed that the Si-O group is at wavelengths of 465 to 475 cm $^{-1}$, the Si–OH group at 800 to 870 cm $^{-1}$, and the siloxane Si-O-Si group at 1115 to 1050 cm $^{-1}$. The O-H molecule group at 1625 cm $^{-1}$ and the O-H group at 3000 to 4000 cm $^{-1}$ [11-13].

3.1.3. XRD

X-ray diffraction (XRD) analysis was carried out to check the formation of the samples. The powder samples were scanned by means of X-ray diffraction using a PW 1800 X-ray Diffractometer, with CuK radiation operating at 40 kV, 30 mA and using Bragg–Brentano geometry at room temperature, 25°C. The spectra are shown in **Fig. 2** for both concentrations of 0.1% and 0.7%, and the average grain particle size of the powder was estimated from the line broadening of the XRD peaks using Scherrer's formula [14]. The average grain size of the powder was found to be close to 41 nm for 0.1% and 39 nm for 0.7%. ***3.2. Annealing treatment***

To prepare a new thermoluminescent material to be used for dosimetric applications, it is necessary to perform a thermal treatment process, usually called annealing. Annealing is carried out in an oven by heating the TL samples up to a given temperature, keeping them at this temperature for a given period of time, and then cooling the samples down to room temperature [15]. This is to stabilize the trap structure and to restore it to its condition prior to irradiation. The annealing processes are required to clear the luminescence traps of residual signals that may cause unwanted background readings during the subsequent use of the material. In general, the annealing treatment has three main goals: (a) to find a good combination of annealing temperature and time to erase any effect of previous irradiation; (b) to produce the lowest intrinsic background and the highest sensitivity. (c) to obtain the highest reproducibility for both TL and background signals. **Fig. 3** shows that the highest TL intensity was detected at 400 °C followed by 200 °C, 300 °C, and 100 °C for 0.1%, and the highest TL intensity was detected at 300 °C followed by 200 °C, 100 °C, and 400 °C for 0.7%. **Fig. 4** indicates the TL response and standard deviation as a function of annealing time for a 400 °C annealing temperature. This means that annealing at 400 °C for 2 hours is more than enough to maximize the emptying of shallow traps and boost electrons out of the traps.

Table 1: Chemical compositions

Compound	Wt %	
	Natural Clay	After Synthesis
SiO_2	63.10	94.10
Al_2O_3	27.10	1.870
Fe_2O_3	5.710	0.484
TIO_2	2.020	-
K_2O	0.633	-
Ca O	0.482	-
SO_3	0.350	0.255
Na_2O	-	2.780

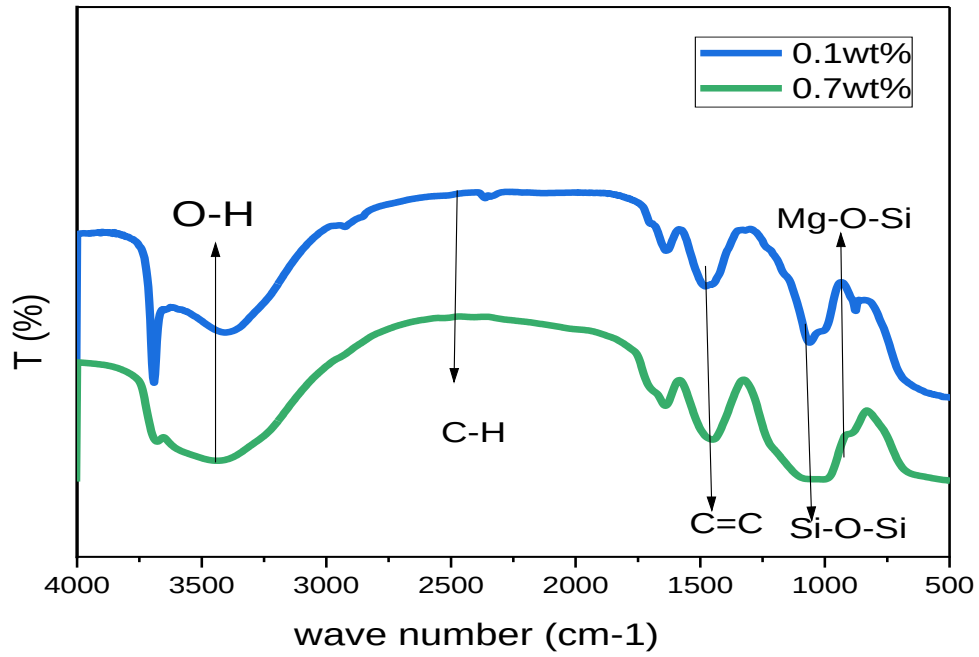

Fig. 1. FTIR spectra for $MgOSiO_2$ 0.1% & 0.7%

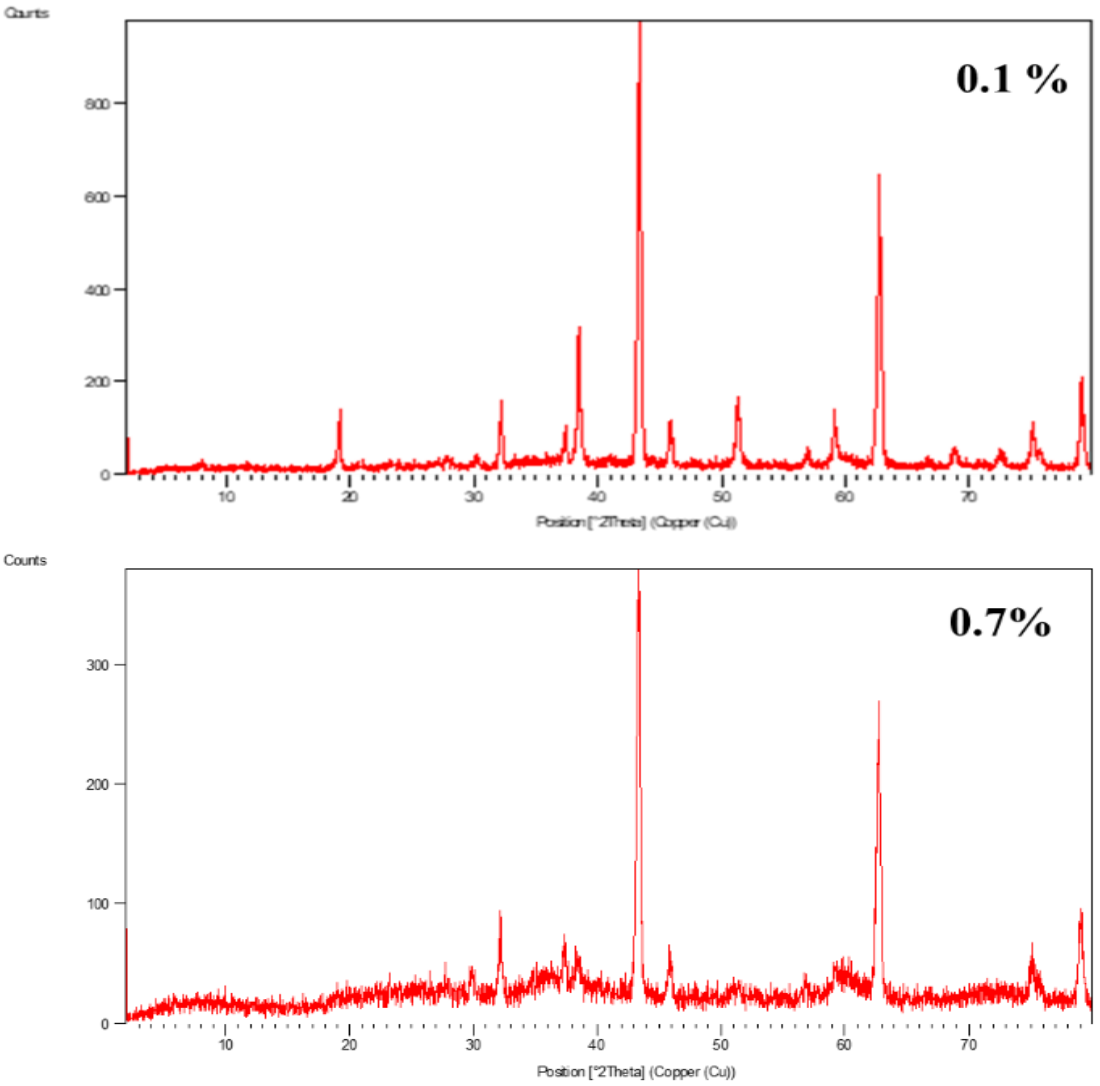

Fig. 2. XRD spectrum for $MgOSiO_2$ (0.1% & 0.7% SiO_2)

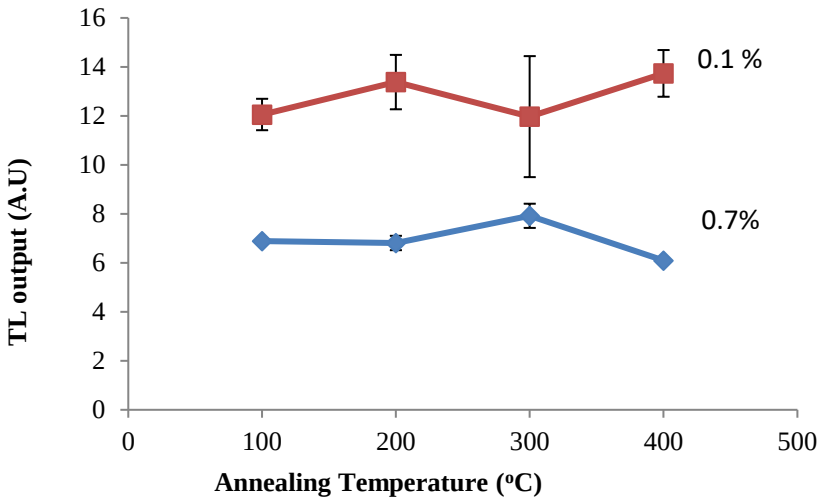

Fig. 3. TL response as a function of annealing temperature at 2h annealing time

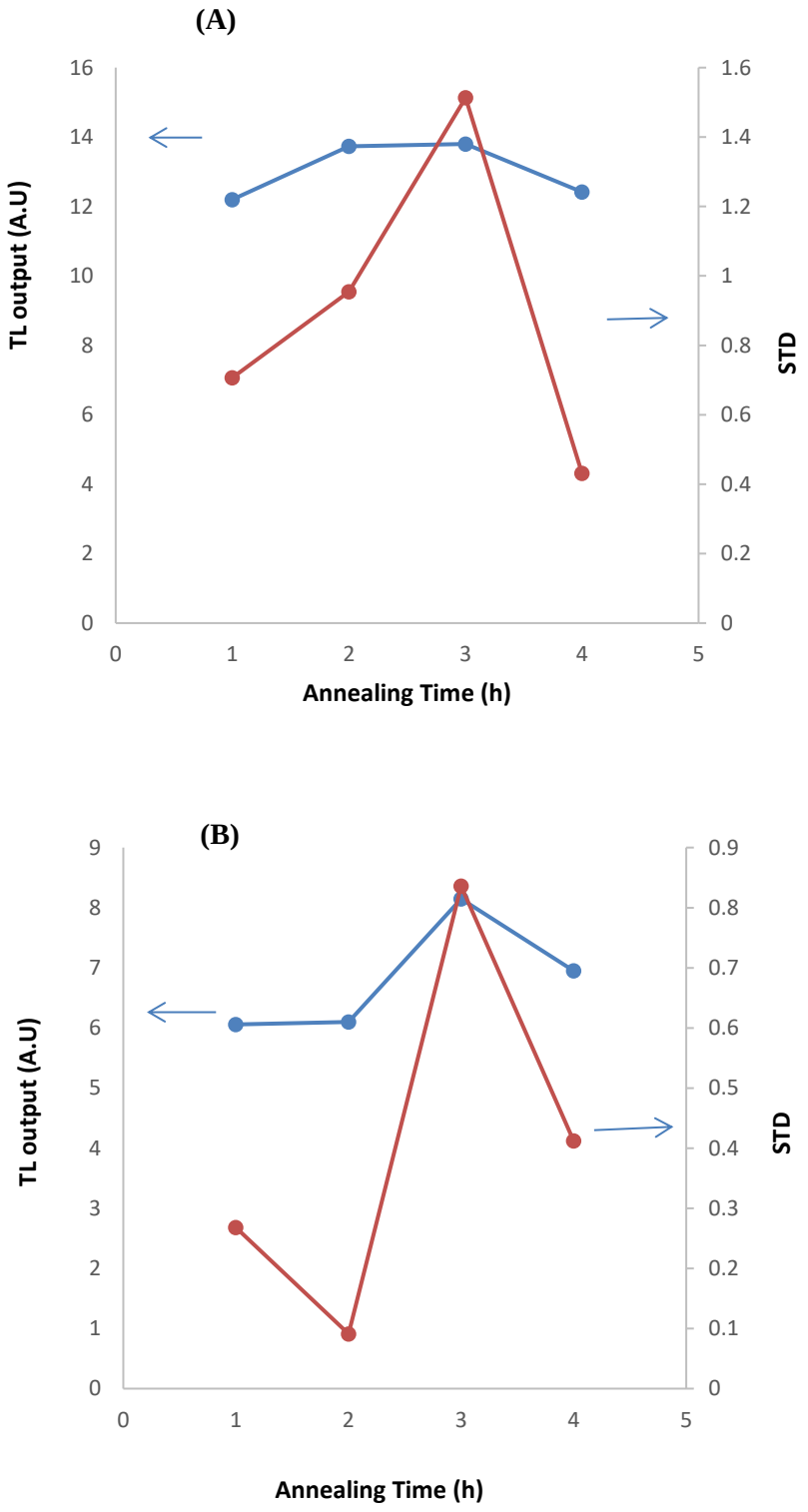

Fig. 4. TL response and the corresponding standard deviation as a function of annealing time at 400°C for (A) 0.1% SiO_2 and (B) 0.7% SiO_2.

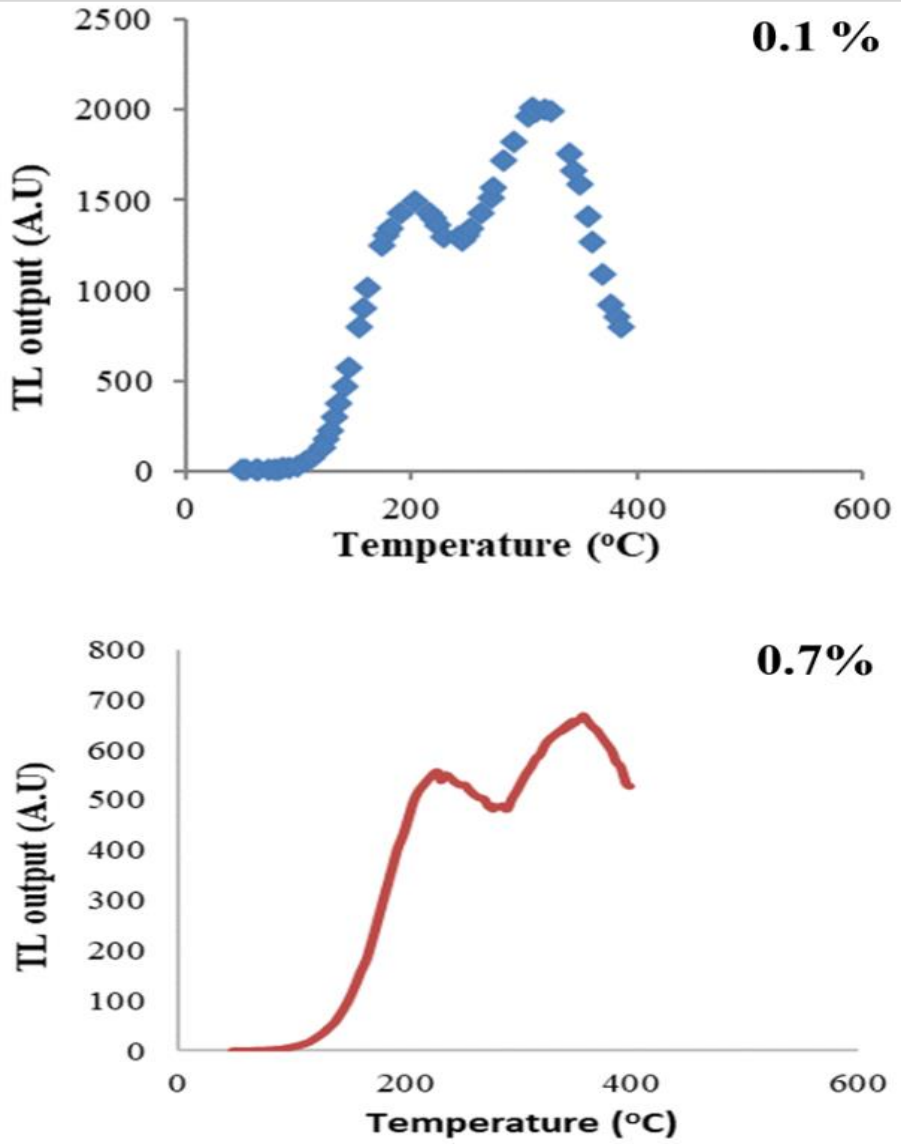

Fig. 5. The characteristic glow curve of $MgOSiO_2$ (0.1% & 0.7%).

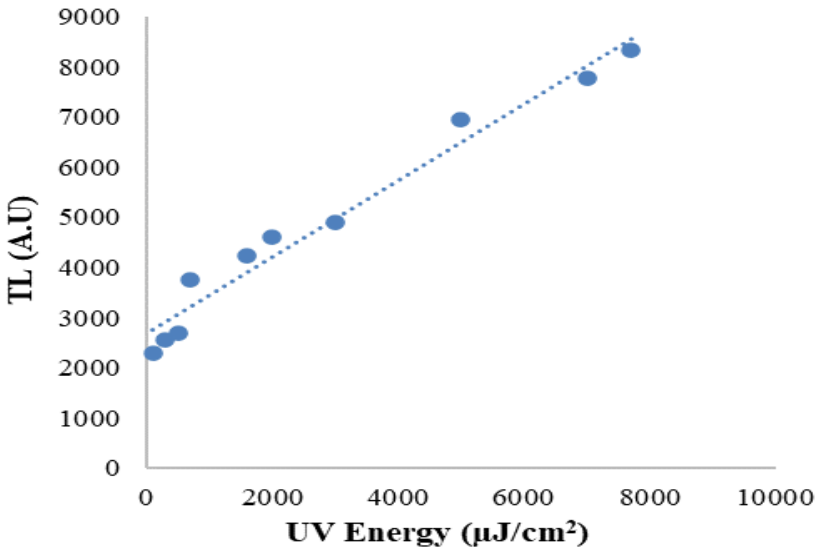

Fig. 6. Energy response for $MgOSiO_2$ (0.1%) after exposure to different UV energy

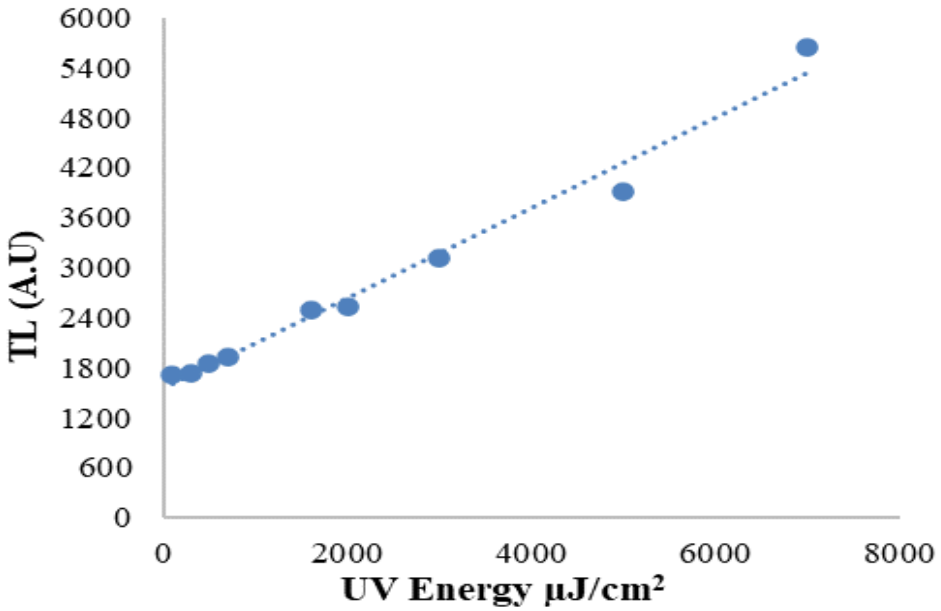

Fig 7. Energy response for $MgOSiO_2$ (0.7%) after exposure to different UV energy

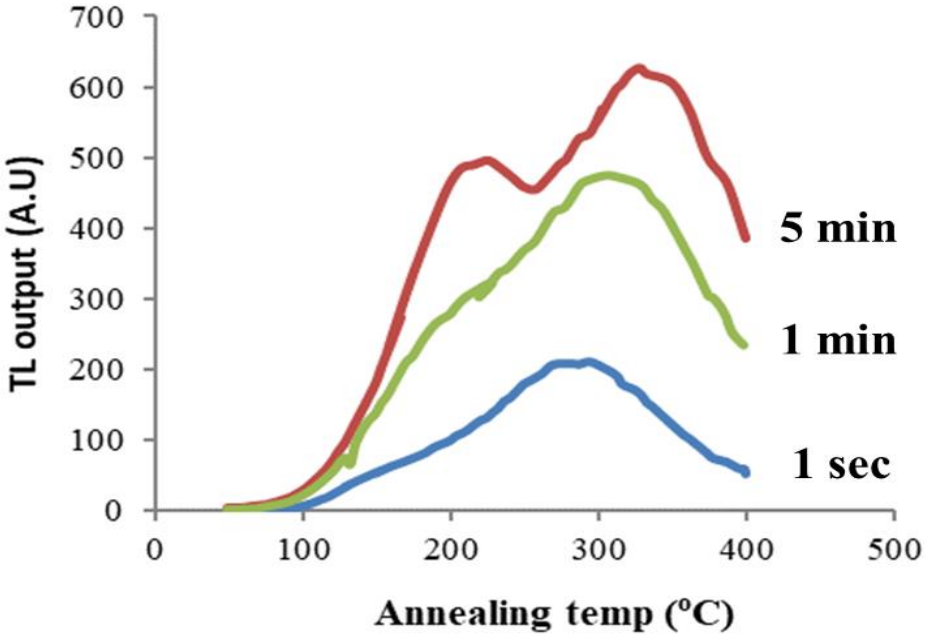

Fig 8. The glow curve of $MgOSiO_2$ for 1sec, 1 min, and 5 min radiation time

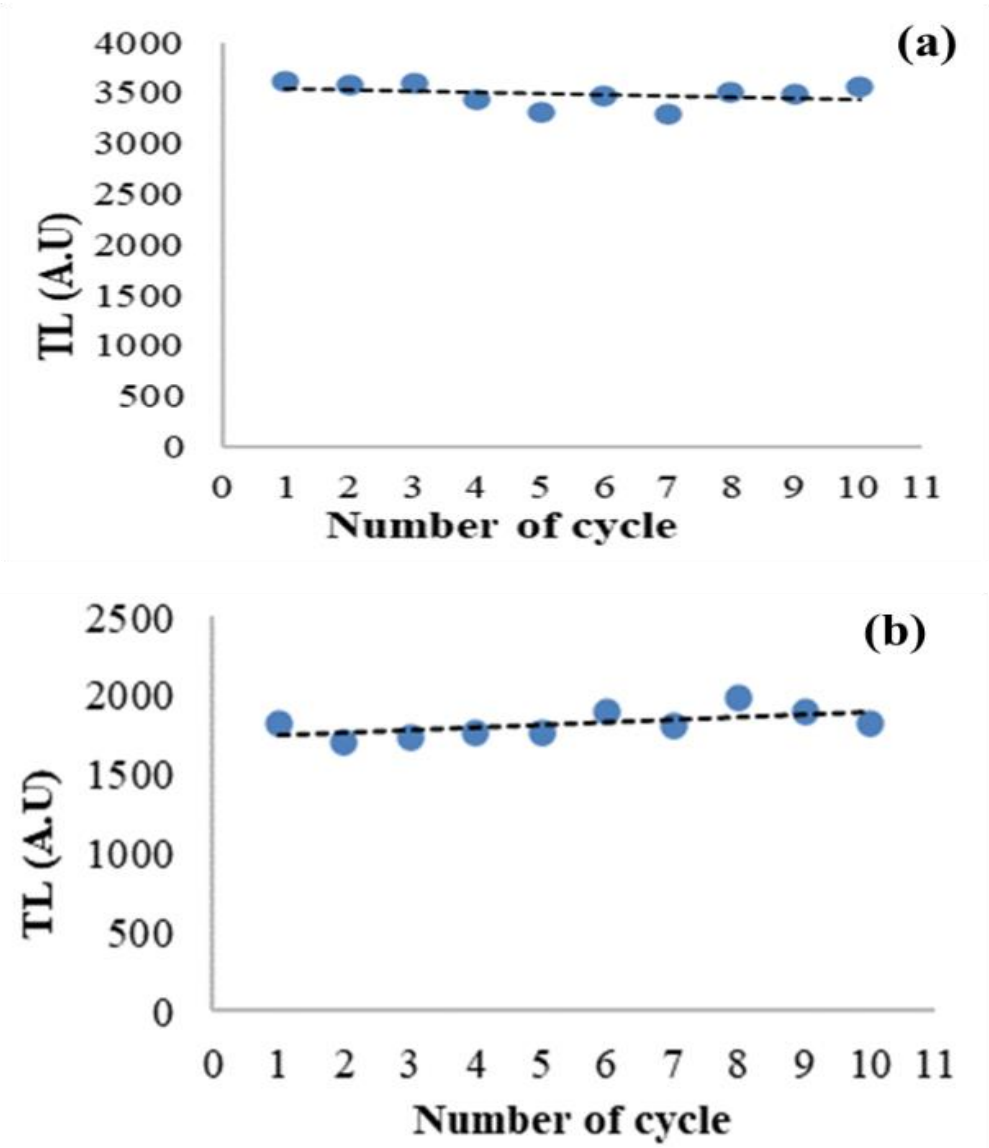

Fig. 9. The reproducibility for (a) 0.1 % $MgOSiO_2$ (b) 0.7 % $MgOSiO_2$

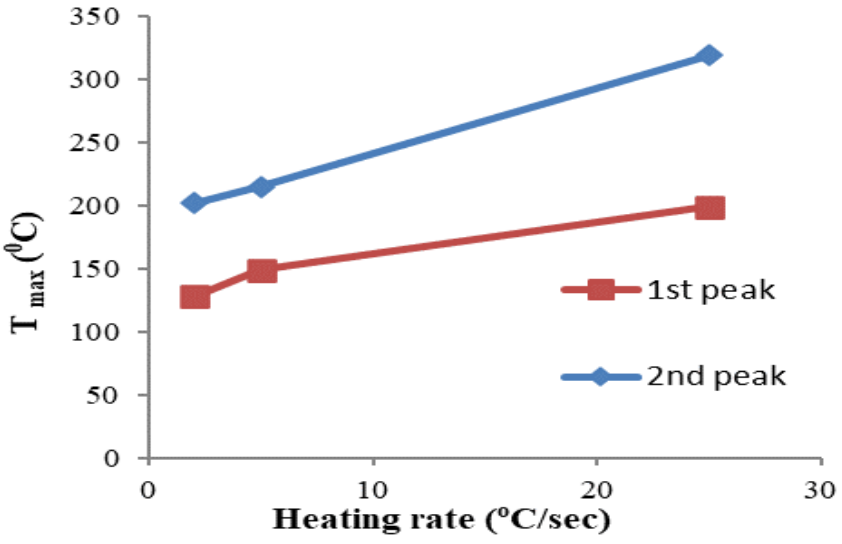

Fig 10. The relation between the heating rate and peak temperature (T_{max}).

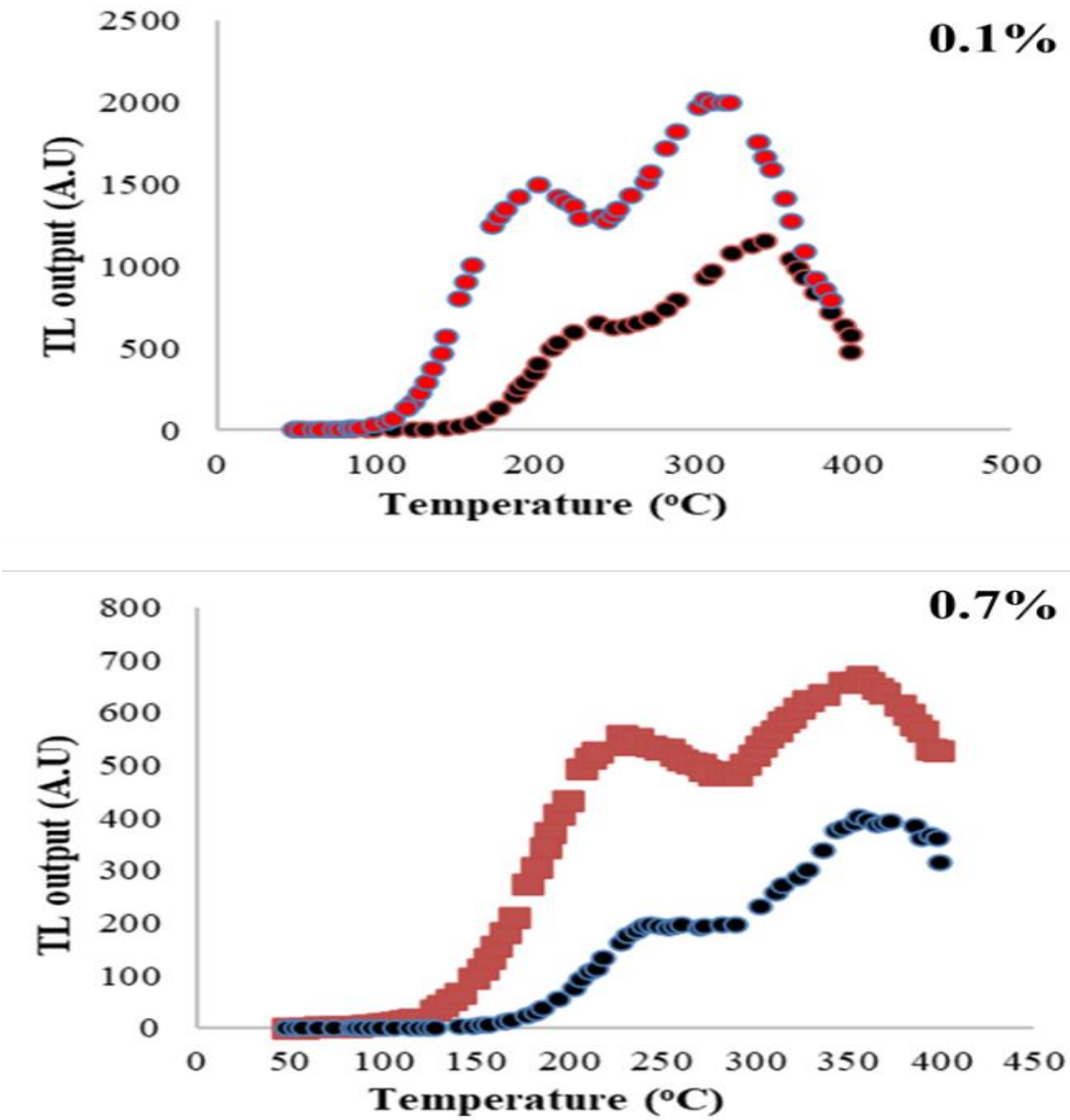

Fig 11. The fading curve after 0 h & 16 days for 0.1% & 0.7%

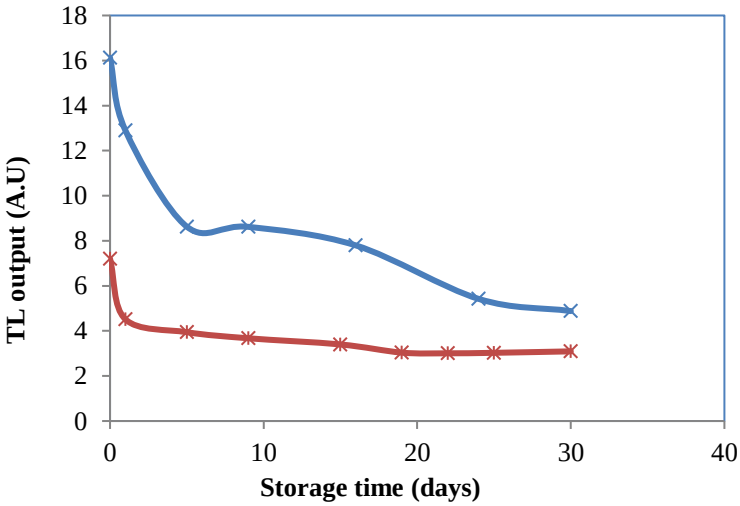

Fig. 12. Fading for 0.1% & 0.7% $MgSiO_2$ from 0 h up to 30 days after UV- irradiation

3.3. TL glow curve

The glow curve is one of the important features for a better understanding of TL phenomena which plots light intensity against the temperature. The shape and position of the glow curve reveal the type of trapping states and their fading characteristics of the corresponding material. Each glow peak is ascribed to the recombination centres and is related to the traps [16]. **Fig. 5** shows the glow curves for $MgOSiO_2$ (0.1%) and $MgOSiO_2$ (0.7%) after being exposed to UV radiation. The area under the glow curve represents the energy distribution of TL carriers. This distribution results from the contribution of electrons ejected from surface defect sites, while the maximum number of electron traps released is indicated by the peak height.

The two main glow peaks can be seen, the low-temperature first peak appears at 203ºC for 0.1% and at 236 °C for 0.7%, and the second peak appears at 307ºC for 0.1% and at 357 °C for 0.7%. Repetitive cycles of annealing and irradiation at the same energy give the same glow curve structure, and when the energy changes, increasing or decreasing, the structure of the glow curve remains the same. It is well known that the ideal glow curve should have a single sharp peak positioned between 180ºC and 250ºC [17].

3.4. Dose–response

The dose–response behavior of $MgOSiO_2$ was studied. The $MgOSiO_2$ sample with two concentrations was exposed to a UV source between 100 J/cm^2 and 7700 J/cm^2. Any material to be used for practical applications needs to have a linear dose pattern. For this purpose, in order to observe the dose behavior of the $MgOSiO_2$, a graph of the total TL glow-curve area versus the UV energy is plotted. **Fig. 6** and **7** show the linear response behavior of the $MgSiO_2$ (0.1% and 0.7%). It is clear from **Fig. 6 & 7** that there is a perfect linear relationship between 100 and 7700 J/cm^2 with correlation coefficients (R^2), which came out to be 0.97 and 0.98 for the concentration of 0.1% & 0.7%. **Fig. 8** shows that the glow curve structure remains the same when the exposure time is increased. The findings show that the slope of the fitted line was approximately 1, which suggests that $MgOSiO_2$ samples show linear behavior.

3.5. Repeatability

Repeatability is one of the most important characteristics and another very useful property when considering practical applications of the phosphor samples [18]. The coefficient of variation (CV) of TL-response for a particular dosimeter that undergoes the same treatment should not exceed 7.5% [18-19]. In order to study the repeatability of the $MgOSiO_2$ sample at a UV energy of 100 J/cm^2, the test was conducted for 10 consecutive cycles of thermal annealing, irradiation, and reading with the same conditions for each annealing cycle to test its repeatability as illustrated in **Fig. 9** and the value of CV was obtained by using Equation (1).

$$CV = \left(\frac{STD}{M}\right) x100 \rightarrow (1)$$

Where, M is the average of the readouts, and STD is the standard deviation. The CV values of $MgOSiO_2$ (0.1%) is 2.3% and for $MgOSiO_2$ (0.7%) is 3.6%, which are lower than the recommended value (7.5%).

3.6. Heating rate

The radiation dosimetric achievement of a TL material strongly relies on the structure of its glow curve, such as maximum TL-intensity and position of glow peaks [1]. Many researchers have used different heating rates to study glow curves for TLD materials. For example, Samei et al. used different heating rates up to 40ºC/sec, Sabini et al. used a heating rate of 15ºC/sec, and Yazici used 1–50ºC/sec [20-22]. **Fig. 10** shows the TL intensity of $MgOSiO_2$ recorded at three heating rates of 2, 5, and 25ºC/sec at 100 J/cm^2 UV energy. The TL glow curves tend to shift toward the higher temperature regions as the heating rate increases. There was a shift of the temperature at the maximum intensity of the glow peak (T_{max}) from low temperature 128 °C to high temperature 199 °C at a heating rate of 2 °C/sec to 25 °C/sec for the 1st peak and from 202ºC to 319ºC for the 2nd peak.

3.7. Fading

Fading is an undesirable decrease in light output that occurs between the irradiation and readout of a TLD. Fading is most likely to involve shallow traps where the energy required to free electrons is the least. As such, the peaks on the glow curve produced at low temperatures can be expected to show the most fading. To study the fading of $MgOSiO_2$ for both concentrations of 0.1% and 0.7%, 30 samples from each concentration were previously annealed, then they were irradiated at 600 J/cm^2 for 5 min, and they kept stored all the time at room temperature (25ºC). Reading was taken at different times starting with 0h up to 600h.

In **Fig. 11**, which shows the fading for both 0.1% and 0.7% at 0 h and 384 h, it is observed clearly the decrease in the intensity of the peaks, and the first peak had a higher fading for both concentrations. **Fig. 12** shows the fading curve for 0.1% and 0.7% $MgOSiO_2$ after 25 days of storage time. The fading is about 66% in a period of up to 25 days for 0.1%, and the first peak area showed about 56% fading in 16 days, and the second peak has about 42% fading in 16 days. The fading is about 57% in a period up to 25 days for 0.7%. The first peak area showed around 64% fading in 16 days, and the second peak showed about 37% fading in 16 days.

4. Conclusions

The SiO_2 was successfully extracted from clay by the sol-gel method and mixed with MgO. The grain size of the mixture was found to be close to 41 nm for 0.1% and 39 nm for 0.7%. The prepared sample has two dosimetric peaks. Depending on the concentration of SiO_2, the first peak appears at 203 ºC and 307 ºC for 0.1%, and 236 °C and 357 °C for 0.7%. The main dosimetric properties such as annealing treatment, reproducibility, dose response, and fading were studied in this work, show that the $MgOSiO_2$ can be used for UV-dosimetry, taking into account their thermal decay at room temperature.

References

[1] C. Furetta. (2010). Handbook of thermoluminescence. World Scientific.

[2] V. Pagonis, G. Kitis, & C. Furetta. (2006). Numerical and practical exercises in

thermoluminescence. Springer Science & Business Media.

[3] S. Guggenheim, & R. T. Martin. (1995). Definition of clay and clay mineral: joint report of the AIPEA nomenclature and CMS nomenclature committees. Clays and clay minerals. 43: 255-256.

[4] F. Bergaya, & G. Lagaly. (2013). Handbook of clay science. Newnes.

[5] C. Woda, T. Schilles, U. Riser, A. Mangini, & G. A. Wagner. (2002). Point defects and the blue emission in fired quartz at high doses: a comparative luminescence and EPR study. Radiation protection dosimetry. 100 (1-4): 261-264.

[6] N. O. Egbe, B. Heaton, & S. McCallum. (2010). Clay as Thermoluminescence Dosemeter in diagnostic Radiology applications. Nigerian Journal of Medicine. 19 (2).

[7] F. A. Balogun, J. O. Ojo, F. O. Ogundare, M. K. Fasasi, & L. A. Hussein. (1999). TL response of a natural fluorite. Radiation measurements. 30 (6): 759-763.

[8] F. O. Ogundare, F. A. Balogun, & L. A. Hussain. (2004). Kinetic characterization of the thermoluminescence of natural fluorite. Radiation measurements. 38 (3): 281-286.

[9] F. O. Ogundare, & M. L. Chithambo. (2006). Accuracy of the activation energy calculated from a thermoluminescence glow-peak using a method that uses three points on the peak. physica status solidi c. 3 (2): 355-361.

[10] C. E. Mokobia. (2012). A study of the thermoluminescence fading characteristics of natural marble phosphor. Scientia Africana. 11 (2).

[11] P. K. Jal, M. Sudarshan, A. Saha, S. Patel, & B. K. Mishra. (2004). Synthesis and characterization of nano silica prepared by precipitation method. Colloids and Surfaces A: Physicochemical and Engineering Aspects: 240 (1-3): 173-178.

[12] M. Waseem, S. Mustafa, A. Naeem, K. H. Shah, I. Shah, & Ihsan-UL-haque. (2009). Synthesis and characterization of silica by sol-gel method. Journal of Pak Mater Society. 3 (1): 19.

[13] M. Waseem, S. Mustafa, A. Naeem, K. H. Shah, I. Shah, & Ihsan-UL-haque. (2009). Synthesis and characterization of silica by sol-gel method. Journal of Pak Mater Society. 3 (1): 19.

[14] I. A. Rahman, P. Vejayakumaran, C. S. Sipaut, J. Ismail, & C. K. Chee. (2008). Effect of the drying techniques on the morphology of silica nanoparticles synthesized via sol–gel process. Ceramics International. 34 (8): 2059-2066.

[15] N. Mandlik, P. D. Sahare, M. S. Kulkarni, B. C. Bhatt, V. N. Bhoraskar, & S. D. Dhole. (2014). Study of TL and optically stimulated luminescence of K2Ca2 (SO4) 3: Cu nanophosphor for radiation dosimetry. Journal of luminescence. 146: 128-132.

[16] Y. Zhang, S. Jin, Y. Yang, C. Liao, & C. Yan. (2002). Annealing effects on the phase and microstructure transformations of nanocrystalline (ZrO2) 1− x (Sc2O3) x (x= 0.02–0.16) thin films deposited by sol–gel method. Solid state communications. 122 (7-8): 439-444.

[17] C. Furetta, S. Guzmán, B. Ruiz, and E. Cruz-Zaragoza. (2011). Retraction notice to “The initial rise method extended to multiple trapping levels in thermoluminescent materials.” Applied Radiation and Isotopes. 9 (69): 346-349.

[18] T. Y. Lim, H. Wagiran, R. Hussin, & S. Hashim. (2015). Thermoluminescence response of dysprosium doped strontium tetraborate glasses subjected to electron irradiations. Applied Radiation and Isotopes. 102: 10-14.

[19] D. Groh, F. Döhler, & D. S. Brauer. (2014). Bioactive glasses with improved processing. Part 1. Thermal properties, ion release and apatite formation. Acta biomaterialia. 10 (10): 4465-4473.

[20] E. Samei, K. J. Kearfott, C. C. Wang, & S. Han. (1994). Impact of variations in physical parameters on glow curves for planchet heating of TL dosimeters. Nuclear Instruments and Methods in Physics Research Section A: Accelerators, Spectrometers, Detectors and Associated Equipment. 353 (1-3): 415-419.

[21] M. G. Sabini, M. Bucciolini, G. Cuttone, A. Guasti, S. Mazzocchi, & L. Raffaele. (2002). TLD-100 glow-curve deconvolution for the evaluation of the thermal stress and radiation damage effects. Nuclear Instruments and Methods in Physics Research Section A: Accelerators, Spectrometers, Detectors and Associated Equipment. 476 (3): 779-784.

[22] A. N. Yazici. (2004). The influence of heating rate on the TL response of the main glow peaks 5 and 4+ 5 of sensitized TLD-100 treated by two different annealing protocols. Nuclear Instruments and Methods in Physics Research Section B: Beam Interactions with Materials and Atoms. 215 (1-2): 174-180.